ELSEVIER

S1359-835X(96)00031-0

Composites Part A **27A** (1996) 633–640
Copyright © 1996 Elsevier Science Limited
Printed in Great Britain. All rights reserved
1359-835X/96/$15.00

Analysis of forming loads for thermoplastic composite laminates

S. R. Morris* and C. T. Sun†
School of Aeronautics and Astronautics, Purdue University, West Lafayette, IN 47907-1282, USA

Using Mindlin plate theory, a model for the forming of thermoplastic composite laminates is presented. The transverse strain in the plate theory is used to account for the slippage between adjacent plies. This interply slip is characterized by a rate dependent constitutive model that is adopted from an experimentally determined relation between the interply shear stress and interply slip velocity. A laminate under cylindrical bending assumptions is used to demonstrate the methodology and to examine the contributions of temperature and loading rate to the amount of compressive stress in the surface ply located on the inner radius of curvature. An experiment which allows measurement of the load histories required to form a thermoplastic composite laminate by the matched die molding process is described. Load histories for two laminates and two forming rates at a typical melt-phase forming temperature are presented along with the histories given by the forming model. Using a hydraulic hot press and two-stage matched die mold, the upper limit on forming rate at a specific forming temperature is demonstrated. Forming above this rate results in wrinkling of the plies on the inner radius of curvature. Copyright © 1996 Elsevier Science Limited

(Keywords: thermoplastic composites; forming; interply slip)

INTRODUCTION

A noted advantage of fiber-reinforced thermoplastic composite materials when compared to similar thermoset systems is their potential for manufacturing structural components at a reduced cost. The absence of complex chemical reactions in the processing of a thermoplastic composite laminate allows it to be formed using processes such as matched die molding, die-less forming, and diaphragm forming. During part fabrication, the material will be subjected to loadings to which the response can no longer be characterized as linearly elastic, and which will, in many instances, result in large interply displacements. In order to predict the response of the laminate to various forming situations, analytical tools are needed to describe the non-linear and rate dependent behavior at typical forming temperatures.

Analyses of the forming process thus far have either modeled the laminate with a layer by layer method, which includes separate layers for the resin rich region and fiber-dominated plies[1,2], or with an approach based on the concept of a fiber-reinforced viscous liquid[3–7]. In the former category, Tam and Gutowski[2] modeled the laminate by elastic composite layers separated by thin viscous resin layers. The viscous resin layers were employed to account for interply slippage. The model was used to analyze an isothermal three-point bending of a unidirectional thermoplastic composite part and was found to compare well with the experimental data. In the fiber-reinforced viscous liquid model, no separate resin rich layers are assumed. Rather, the matrix is assumed to be a linear viscous liquid whose motion is constrained by inextensible fibers.

The approach presented here is motivated by the observation that the transverse shear deformation of a laminate experienced during forming is the result of interply slippage. Hence, interply slippage may be conveniently modeled by transverse shear deformation of the laminate. Evidently, a laminate theory such as Mindlin plate theory[8,9] that accounts for transverse shear deformation must be used for such a purpose. For such a model, the behavior of the transverse shear deformation of the laminate must be related to the behavior of interply slip. The main advantage of the present model is the possibility of using commercially available finite element codes to perform the analysis. This is particularly attractive for complex geometries and forming conditions.

*Current address: United Technologies, Pratt & Whitney, East Hartford, CT 06108, USA
†To whom correspondence should be addressed

ClearCorrect Exhibit 1165, Page 1 of 8
ClearCorrect v. Align - IPR2025-00821

In this paper, the proposed model is used to analyze the deformation of AS4/PEEK thermoplastic composite laminates under three-point bending. Various stroke rates and temperatures are considered. Analytical results are compared with experimental data.

CONSTITUTIVE MODELS

The composite is modeled as an elastic–viscoplastic solid. The elastic part of the strain follows linear stress–strain relations for orthotropic elastic solids. A two-dimensional (2-D) viscoplastic constitutive model proposed by Gates and Sun[10] is adopted to describe the in-plane viscoplastic behavior. For a state of plane stress, the plastic strain rates are obtained by the associated flow rule:

$$\{\dot{\varepsilon}^{\mathrm{p}}\} = \dot{\bar{\varepsilon}}^{\mathrm{p}} \frac{\partial \bar{\sigma}}{\partial \{\sigma\}} \tag{1}$$

where $\dot{\bar{\varepsilon}}$ is the effective plastic strain rate and $\bar{\sigma}$ is the effective stress defined by

$$\bar{\sigma} = \sqrt{3f} \tag{2}$$

In the above equation f is the one parameter plastic potential given by

$$2f = \sigma_{22}^2 + 2a_{66}\sigma_{12}^2 \tag{3}$$

in which a_{66} is a parameter associated with the anisotropy of the material. The functional form of the effective plastic strain rate is

$$\dot{\bar{\varepsilon}}^{\mathrm{p}} = \left(\frac{H}{K}\right)^{1/m} \tag{4}$$

where K and m are material constants, and H is the overstress which is defined as the difference between the instantaneous effective stress and the effective quasistatic stress corresponding to the same value of effective plastic strain. The effective quasistatic stress–effective plastic strain curve is considered to be the limiting case (vanishing strain rate) of the viscoplastic stress–strain curve and is given by the hardening rule

$$\bar{\varepsilon}^{\mathrm{p}} = B(\bar{\sigma}*)^{\eta} \tag{5}$$

where B and η are material constants, and $\bar{\sigma}*$ is the effective quasistatic stress.

Since the majority of forming operations involve interply slip, a constitutive model for the transverse shear response of the laminate is developed based on the experimental study of interply slip behavior by Morris and Sun[11] in the AS4/PEEK composite material system for the temperature range characteristic of both the solid-phase and melt-phase forming processes. The interfacial shear stress was shown to have the following power law behavior with respect to the interply slip velocity[11]:

$$\tau = Av^n \tag{6}$$

where τ is the magnitude of the shear stress and v is the interply slip velocity. The coefficient A and exponent n are both dependent on temperature. Power law behavior was noted for the relationship between A and the temperature, while n behaved linearly with variation in temperature. For the same interfacial slip velocity, higher shear stress values were observed for axial interfaces, interfaces between plies of like orientation, than for non-axial interfaces, interfaces between plies of different orientations.

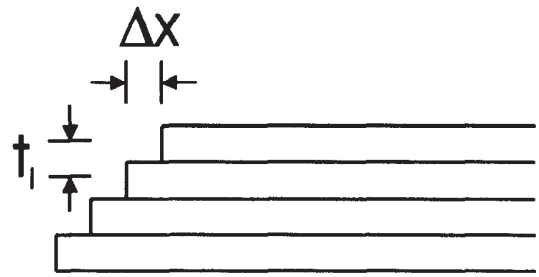

Figure 1 One-dimensional ply slip relationship

A yield stress, which had to be exceeded before the steady-state slip behavior began, was observed. The yield stress demonstrated the same dependencies on slip velocity, temperature, and interface orientation as did the steady state. The value of the yield stress is considerably higher than the steady state value in the solid-phase forming temperature range. This difference decreases with increasing temperature, and the magnitude of the yield stress becomes less than the value of stress required for steady-state slip at temperatures in the melt-phase forming range. The equivalent temperature, the temperature at which the values of the yield and steady-state stress are equal for a given interply slip rate, marks the transition from solid-phase forming to melt-phase forming.

Since the experimental model of the interply slip mechanism is in terms of interply slip velocity, a relation between this velocity and the appropriate strain rate is necessary. The stresses in the plane of the interface are the transverse shear stresses τ_{xz} and τ_{yz}, and the corresponding strains are γ_{xz} and γ_{yz} where x and y are the coordinate axes in the plane of the interface, and z is in the normal direction. It can be shown that the magnitude of the resultant shear stress in the plane of the interface is

$$\bar{\tau} = \sqrt{\tau_{xz}^2 + \tau_{yz}^2} \tag{7}$$

and that the corresponding resultant transverse shear strain rate magnitude is

$$\dot{\bar{\gamma}}^{\mathrm{p}} = \sqrt{(\dot{\gamma}_{xz}^{\mathrm{p}})^2 + (\dot{\gamma}_{yz}^{\mathrm{p}})^2} \tag{8}$$

Considering the geometry shown in *Figure 1* for a one-dimensional slip case, the relation between the resultant transverse shear strain and the magnitude of slip in the

ClearCorrect Exhibit 1165, Page 2 of 8
ClearCorrect v. Align - IPR2025-00821

same direction is

$$\bar{\gamma} = \frac{\Delta x}{t_1} \tag{9}$$

where Δx is the slip distance at an interface and t_1 is the distance between the midpoints of two adjacent plies and is equal to the ply thickness. The corresponding relation between interply slip velocity and resultant transverse shear strain rate at the interface is

$$\dot{\bar{\gamma}}^{\mathrm{p}} = \frac{\bar{v}}{t_1} \tag{10}$$

where $\bar{v}$ is the magnitude of the resultant interply slip velocity.

By using the relation between $\bar{\tau}$ and $\bar{v}$, the resultant transverse shear strain rate can be related to the resultant shear stress as

$$\dot{\bar{\gamma}}^{\mathrm{p}} = \frac{1}{t_1}\left(\frac{\bar{\tau}}{A}\right)^{1/n} \tag{11}$$

Thus, the interply slip is modeled as the transverse shear strain of the laminated plate.

The rate dependent transverse shear behavior can be modeled in a manner similar to the in-plane deformation. We define a plastic potential for transverse shear as

$$2f^{\mathrm{T}} = \tfrac{1}{3}(\tau_{xz}^2 + \tau_{yz}^2) \tag{12}$$

The components of the transverse shear strain rate can be derived using the associated flow rule of equation (3) with the appropriate expressions for transverse shear.

$$\begin{Bmatrix} \dot{\gamma}_{xz}^{\mathrm{p}} \\ \dot{\gamma}_{yz}^{\mathrm{p}} \end{Bmatrix} = \frac{1}{t_1}\left(\frac{\bar{\tau}}{A}\right)^{1/n} \begin{Bmatrix} \tau_{xz} \\ \tau_{yz} \end{Bmatrix} \Big/ \bar{\tau} \tag{13}$$

There is no quasistatic stress in the plastic transverse shear analysis, meaning that once the yield stress has been exceeded, the total transverse shear contributes to the interply slip deformation.

SIMPLIFIED LAMINATE ANALYSIS

The plate displacements according to Mindlin plate theory are given by

$$u(x,y,z) = z\Psi_x(x,y) \tag{14}$$

$$v(x,y,z) = z\Psi_y(x,y) \tag{15}$$

$$w(x,y,z) = w(x,y) \tag{16}$$

where Ψ_x and Ψ_y are rotations of the cross-sections. The transverse shear strains are

$$\gamma_{xz} = \frac{\partial w}{\partial x} + \Psi_x \tag{17}$$

$$\gamma_{yz} = \frac{\partial w}{\partial y} + \Psi_y \tag{18}$$

The in-plane and the transverse shear constitutive equations presented in the previous section can be used together with the plate displacements to derive the plate constitutive and equilibrium equations for the laminate[12].

Since transverse shear strain is constant across the thickness in Mindlin plate theory[9], it must be assumed that interply slip is dispersed uniformly across the thickness and that only one type of interface behavior is accommodated, i.e. either axial (same fiber orientation between adjacent plies) or non-axial. The limit to one type of interface should not be a problem as most laminates will primarily have non-axial interfaces; however, an averaging of axial and non-axial interface properties could be used in cases where a significant number of each type of interface exists.

Given the extent of material non-linearity and the potential for large deflections, numerical methods will be required to perform the analysis. The finite element formulation presented by Wang *et al.*[12], which utilizes an isoparametric four-noded Mindlin plate finite element developed by Chen[13] for elastic/plastic analysis of plates and shells under large deflection, can be used with the modified transverse shear constitutive model to provide a broad analysis capability. It is also possible to use some of the commercial finite element codes through the use of user subroutine to implement the present constitutive models.

In this study, we consider problems of fiber-dominated composite laminates under three-point bending. For these laminates, their deflections are dominated by the longitudinal modulus of the composite ply, which is basically elastic until interply slip sets in. The transverse shear deformation is assumed to be elastic initially until the stress (beyond which interply slip takes place) is reached. After this point the analysis proceeds according to the viscoplastic constitutive model. In other words, before interply slip occurs, the analysis is elastic. Such a simplifying assumption enables us to obtain analytical solutions for some cylindrical bending problems.

LOAD HISTORY ANALYSIS

An example which lends itself to analysis without extensive use of numerical procedures is a laminated plate which is simply supported on two edges. The deformation of this laminate may be dictated by either a known load history or a known diplacement history. In most press forming operations, a constant displacement rate is maintained during the forming process. This displacement rate can then be used to determine the load history of the laminate. Since fiber buckling on the inner radius of a bend is a major concern during forming, optimizing the forming parameters so that compressive stresses are minimized is desirable.

Consider a symmetric cross-ply laminate with a span L in the x direction and infinite in the y direction. If the loading is a function of x only, then the plate displacements and rotations are also functions of x only, and the deflected surface is cylindrical. The small

ClearCorrect Exhibit 1165, Page 3 of 8
ClearCorrect v. Align - IPR2025-00821

deflection equilibrium equations for this problem are

$$\frac{dQ_x}{dx} + q = 0 \tag{19}$$

$$\frac{dM_x}{dx} - Q_x = 0 \tag{20}$$

where q is the transverse load, and M_x and Q_x are the bending moment and shear force, respectively. The plate constitutive equations are

$$M_x = D_{11}\frac{d\Psi_x}{dx} \tag{21}$$

$$Q_x = A_{55}^{e}\left(\frac{dw^e}{dx} + \Psi_x\right) \qquad \text{elastic} \tag{22}$$

$$Q_x = A_{55}^{vp}\left(\frac{d\dot{w}^p}{dx} + \dot{\Psi}_x\right)^n \qquad \text{viscoplastic} \tag{23}$$

where Ψ_x is the rotation of the cross-section with respect to the y axis, w is the transverse deflection, D_{11} is the bending stiffness of the laminate, A_{55} is the laminate transverse shear stiffness, and superscripts e and vp denote elastic and viscoplastic parts, respectively. The laminate stiffnesses D_{11} and A_{55} are related to the composite properties by

$$D_{11} = \sum_{k=1}^{N} \bar{Q}_{11}^{(k)}(z_{k+1}^3 - z_k^3) \tag{24}$$

$$A_{55}^{e} = hG \tag{25}$$

$$A_{55}^{vp} = hAt_1^n \tag{26}$$

where $\bar{Q}_{11}^{(k)}$ is the reduced stiffness of a lamina in the x direction, z is the distance from the laminate midplane to a lamina, h is the laminate thickness, G is the shear modulus of the composite where it has been assumed that $G_{12} = G_{13} = G_{23} = G$, and A and n are parameters from the interply slip model. The yield point between elastic and viscoplastic behavior for transverse shear is governed by the elastic transverse shear strain rate as

$$\bar{\tau}_Y = A_Y(t_1\dot{\bar{\gamma}}^e)^{n_Y} \tag{27}$$

where A_Y and n_Y are the parameters given in ref. 11.

The boundary conditions of this plate are

$$w = M_x = 0 \qquad \text{at} \qquad x = 0, L \tag{28}$$

$$\Psi_x = 0 \qquad \text{at} \qquad x = L/2 \tag{29}$$

The constraint on the displacement rate is defined by specifying the mid-span displacement rate as

$$\dot{w}\left(\frac{L}{2}\right) = \dot{w}_0 = \text{constant} \tag{30}$$

The elastic material constants of the AS4/PEEK composite material at temperatures above the glass transition temperature were obtained by Wang[14] up to a temperature of 315°C. The longitudinal modulus E_1 and transverse modulus E_2 were obtained directly from the measurement of 0° and 90° specimens. The shear modulus was determined from the off-axis apparent elastic modulus E_x measured for 20°, 30°, 45°, and 60° off-axis specimens using

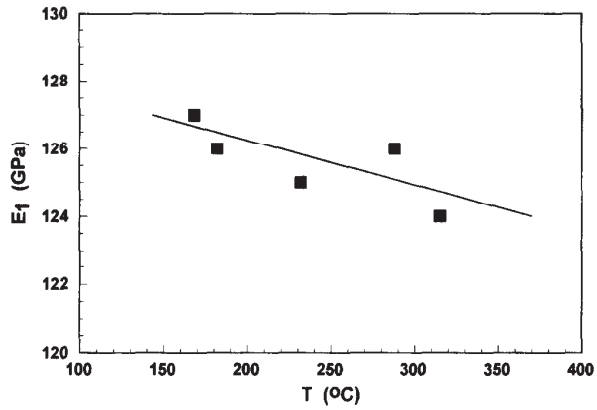

Figure 2 Temperature dependence of E_1 above the glass transition temperature for AS4/PEEK

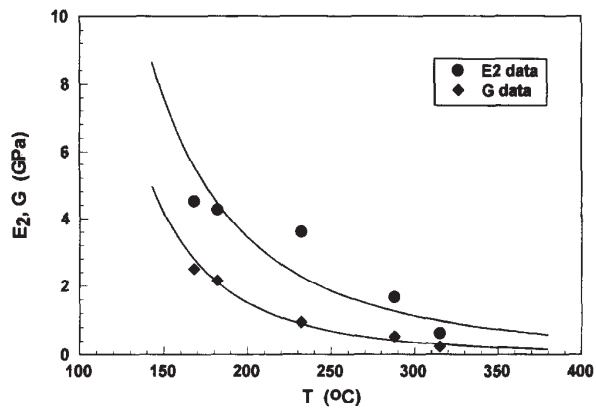

Figure 3 Temperature dependence of E_2 and G_{12} above the glass transition temperature for AS4/PEEK

$$G_{12} = E_2 \sin^2\theta\cos^2\theta \Big/ \left[\left(\frac{E_2}{E_x} - \sin^4\theta\right) + \frac{E_2}{E_1}(2\nu_{12}\sin^2\theta\cos^2\theta - \cos^4\theta)\right] \tag{31}$$

where $\nu_{12} = 0.4$ for temperatures above 200°C is taken from ref. 15.

The variation of E_1 with temperature is small, ranging from 127 GPa at 68°C to 124 GPa at 315°C; E_1 can be modeled by a linear function obtained by the least-squares method as

$$E_1 = 129 - 0.0133T \qquad \text{(GPa)} \tag{32}$$

as shown in *Figure 2*.

The E_2 and G_{12} data are fit with power law relations. Power laws are selected to avoid negative values for these material properties when the data is extrapolated to temperatures representative of forming. The equations for the curve-fits, also obtained by the least-squares

ClearCorrect Exhibit 1165, Page 4 of 8
ClearCorrect v. Align - IPR2025-00821

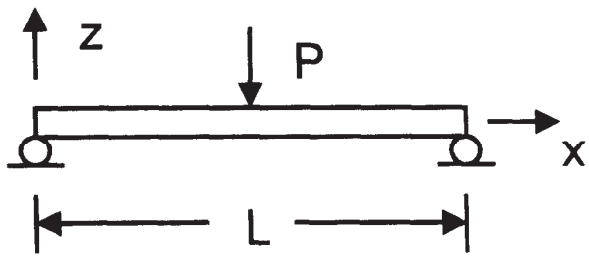

Figure 4 A simply supported, symmetric, cross-ply laminate subject to a concentrated load at mid-span

method, are

$$E_2 = 7.32 \times 10^6 T^{-2.75} \quad \text{(GPa)} \tag{33}$$

$$G_{12} = 2.01 \times 10^8 T^{-3.53} \quad \text{(GPa)} \tag{34}$$

which are shown graphically in *Figure 3*.

The functions given by equations (27)–(29) enable us to extrapolate the elastic moduli beyond 300°C. Since E_1 is dominated by the fiber, such extrapolation should be valid. The same cannot be said with confidence about E_2 and G_{12}. However, in a fiber-dominated laminate, the bending stiffness is dominated by E_1 and the transverse shear property is controlled by interply slip; consequently, some errors in the values of E_2 and G_{12} should not affect the result of the present analysis.

A concentrated is applied at $x = L/2$ as shown in *Figure 4*. This loading is the type which would occur during the initial portion of a matched die molding process. Consider the left half of the laminate. Since there is no distributed load q in this case, the governing equations reduce to

$$\frac{d^2 M_x}{dx^2} = 0 \tag{35}$$

Substituting equation (16) in equation (30) gives

$$\frac{d^3 \Psi_x}{dx^3} = 0 \tag{36}$$

Integrating with respect to x three times and evaluating the constants with the boundary conditions yields

$$\Psi_x = \frac{P}{16D_{11}}(-4x^2 + L^2) \tag{37}$$

Therefore, is is seen that the rotation is governed solely by the elastic in-plane response.

Since the shear force is $P/2$, equation (22) and the displacement boundary condition are used to determine the deflection shape

$$w^e = P\left[\frac{x^3}{12D_{11}} - \left(\frac{L^2}{16D_{11}} + \frac{1}{2A_{55}^e}\right)x\right] \tag{38}$$

Since the displacement rate is a specified constant at mid-span, equation (38) is evaluated at $x = L/2$ and differentiated with respect to time to find that the initial loading rate is

$$\dot{P} = \dot{w}_0\left(\frac{L^3}{48D_{11}} + \frac{L}{4A_{55}^e}\right)^{-1} \tag{39}$$

The effective transverse shear stress is given by

$$\bar{\tau} = \frac{Pt}{2h} \tag{40}$$

The effective elastic transverse shear strain rate is

$$\dot{\bar{\gamma}}^e = \frac{\dot{P}}{2hG} \tag{41}$$

Using equation (27), the time for which the initial loading rate must be applied before interply slip begins is found to be

$$t_Y = A_Y\left(\frac{\dot{P}}{2h}\right)^{n_Y - 1}\left(\frac{t_1}{G}\right)^{n_Y} \tag{42}$$

Now equation (18), the viscoplastic transverse shear constitutive equation, with the appropriate derivative of equation (37), is used to find the expression for the plastic displacement rate of the laminate,

$$\dot{w}^p = \left(\frac{P}{2A_{55}^{vp}}\right)^{1/n} x + \frac{\dot{P}}{4D_{11}}\left[-\frac{x^3}{3} + \left(\frac{L}{2}\right)^2 x\right] \tag{43}$$

Evaluating equation (38) at $x = L/2$ and rearranging yield a non-linear differential equation for the loading rate during viscoplastic deformation,

$$\dot{P} = \frac{48D_{11}}{L^3}\left[\dot{w}_0 - \frac{L}{2}\left(\frac{1}{2A_{55}^{vp}}\right)^{1/n}(P)^{1/n}\right] \tag{44}$$

This non-linear differential equation must be solved by a numerical method such as Newton's method. The plastic displacement rate has been taken to be the total displacement rate since the elastic displacement rate vanishes under steady state viscoplastic deformation.

The compressive normal stress in the surface ply on the inner radius at $x = L/2$ is given by

$$\sigma_{xx} = \frac{\bar{Q}_{11}}{D_{11}}\frac{PL}{4}\left(\frac{N-1}{2}t_1\right) \tag{45}$$

The effect of the displacement rate on the maximum load applied to the laminate at various temperatures is shown in *Figure 5*. The load at a given displacement rate decreases with increasing temperature; however, this difference decreases as the rate increases and becomes zero for temperatures of 340°C and above at around 80 m/s. This rate is exceptionally high and is most likely out of standard processing ranges.

From equation (45), we see that the critical bending stress is proportional to the load shown in *Figure 5*. This stress can be reduced at a given forming temperature by forming at the slowest rate that is feasible. If the forming environment is not isothermal, the part may cool below the desired forming temperature during the time required

ClearCorrect Exhibit 1165, Page 5 of 8
ClearCorrect v. Align - IPR2025-00821

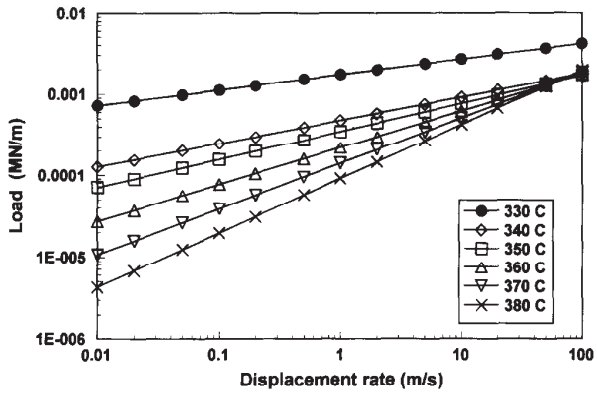

Figure 5 Variation of the load required to maintain a given displacement rate with temperature for the concentrated load forming example

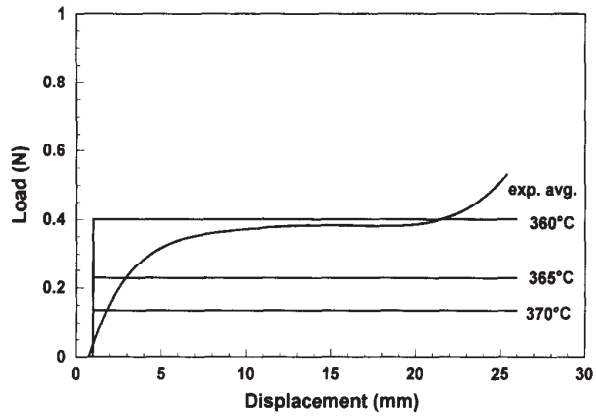

Figure 7 Experimental and model load histories for tests conducted at 2.12 mm/s on $[0/90]_{3s}$ specimens

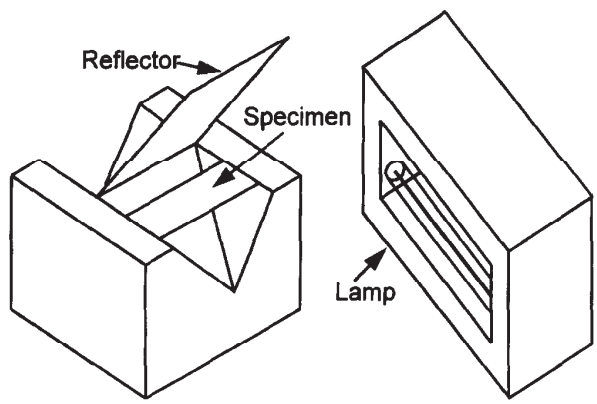

Figure 6 Schematic of the experimental set-up for the measurement of load histories

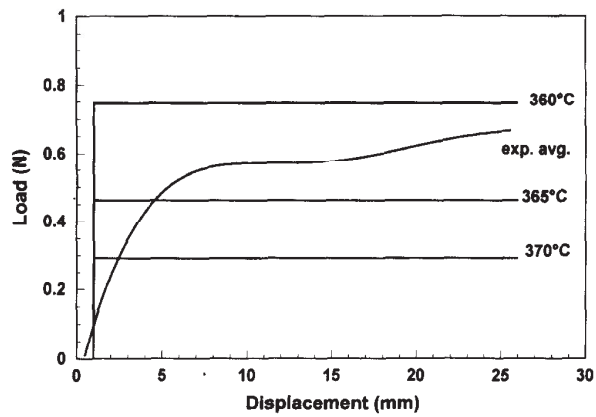

Figure 8 Experimental and predicted load histories for tests conducted at 8.47 mm/s on $[0/90]_{3s}$ specimens

to form the part at a slow forming rate. If the forming requires large displacements, the appropriate large deflection corrections must be applied to this analysis.

EXPERIMENTAL PROCEDURE

In order to verify the load histories resulting from equations (39) and (44), a series of experiments representing three-point bending were conducted. Specimens with dimensions of 73.0 mm by 25.4 mm were cut from preconsolidated $[0/90]_{3s}$ and $[0/90/\pm45]_{2s}$ laminates. The ends of the specimen were placed on the insulated edges of a V-shaped mold cavity as shown in *Figure 6*. To heat the specimen to the desired test temperature of 370°C, a Research Incorporated model 4184-05 infrared strip heater was used. The heater was oriented so that the tubular quartz lamp was parallel to the edge of the specimen. A V-shaped reflector was placed behind the specimen perpendicular to the mold cavity to focus the infrared energy on the laminate. A cylindrical indentor with a diameter of 12.5 mm was used to load the specimen at mid-span. The load was applied by a Sintech 10 screw type universal testing machine with a 44.5 N load cell. Machine operation and data acquisition were accomplished by personal computer. Displacement rates of 2.12 and 8.47 mm/s were specified such that a total displacement of 25.4 mm was achieved.

Small pieces of prepreg were used to attach type K thermocouples to the upper and lower surfaces of the specimen by melting the prepreg with a large soldering iron. An AC power supply was used to control the heat lamp. To heat the specimen, the controller was set to 30% of full power for approximately 5 s, to prolong the life of the tungsten filament in the quartz bulb, before increasing the setting to 60%. The controller remained at 60% until the thermocouples read 232°C. Power was then increased to 80% until the surface temperature of the specimen reached 315°C. Full power was used to raise the temperatures to approximately 370°C at which point the constant displacement rate test was conducted.

RESULTS AND DISCUSSION

Figures 7 and *8* show the results of the slow and fast displacement rate cases for the $[0/90]_{3s}$ laminate, and

ClearCorrect Exhibit 1165, Page 6 of 8
ClearCorrect v. Align - IPR2025-00821

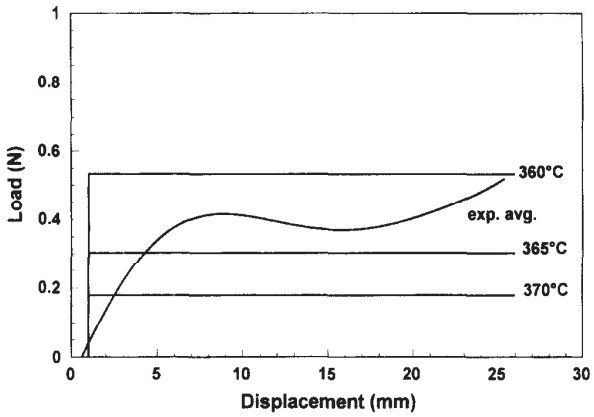

Figure 9 Experimental and predicted load histories for tests conducted at 2.12 mm/s on $[0/90/\pm45]_{2s}$ specimens

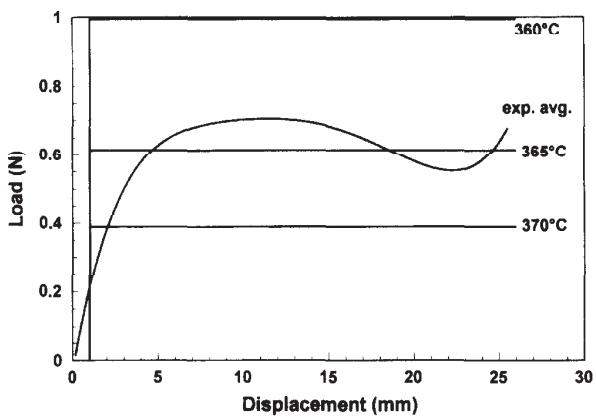

Figure 10 Experimental and predicted load histories for tests conducted at 8.47 mm/s on $[0/90/\pm45]_{2s}$ specimens

Figures 9 and *10* show the results for the same rates with the $[0/90/\pm45]_{2s}$ laminate. On each figure an experimental average of 3–4 tests based upon a sixth-order polynomial is shown, as well as, the loads resulting from the small deflection theory with material properties corresponding to 360, 365, and 370°C. From these predictions it can be seen how sensitive the load history obtained from the forming model is to the temperature. A drop in temperature of less than 3% results in an increase in load of more than 180%.

The experimental results fall between the 360 and 365°C predictions. Although these loads are above the predicted 370°C loads, certain conditions existed in the experiment which were not accounted for in the modeling. It was not possible to control the heat source to maintain a constant temperature for a long period of time; thus, the specimens were not held at 370°C for more than 30 s, and a temperature gradient may have existed through the thickness. Since the indentor was not heated, it would have acted as a heat sink during loading and lowered the temperature of the specimen.

The average initial steady-state loads for the $[0/90]_{3s}$ specimens were 0.33 N for the 2.12 mm/s test rate and 0.53 N for the 8.47 mm/s test rate. Values of 0.39 and 0.65 N were found for the $[0/90/\pm45]_{2s}$ laminate at the 2.12 and 8.47 mm/s test rates, respectively. The ratios of the initial steady-state load at the lower displacement rate with respect to the initial steady-state load at the higher displacement rate show a consistent trend with values of 0.62 for the $[0/90]_{3s}$ specimens and 0.60 for the $[0/90/\pm45]_{2s}$ specimens. The similarity in values for this ratio indicates the same rate dependence for each laminate.

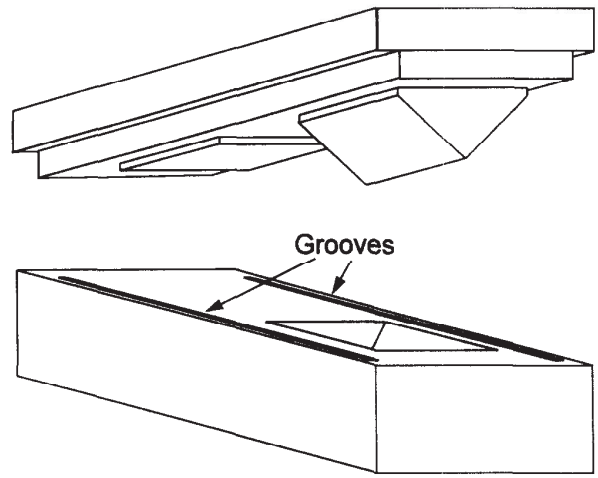

Figure 11 Two-stage matched die mold with right angle forming cavity

FORMING RATE EFFECTS

The matched die molding process was used to investigate the effect an increased loading rate would have on the quality of the part being formed. As was seen in *Figure 5*, our model predicts an increase in the forming load with an increase in forming rate. This increased load could reach a level at which the resulting compressive stress in the plies on the inner radius of curvature could buckle or wrinkle.

A single station hydraulic press, manufactured by Carver and consisting of a pair of platens which are heated to a specified temperature and a pair of platens which are cooled by chilled water, was used. The closure rate of the platens is adjusted by a dial setting between 0 and 10. The maximum setting corresponds to a rate of 13.8 mm/s. This rate is the most commonly used. The force corrsponding to the desired consolidation pressure may also be specified, and an auto setting compensates for any loss of force during processing.

The procedure for forming a part from a preconsolidated laminate requires the laminate to be preheated. Once the heated platens have reached the desired forming temperature, the part to be formed is placed between release film that is attached to a frame which slides between the two halves of the mold as shown in *Figure 11*. The temperature of the laminate is monitored

ClearCorrect Exhibit 1165, Page 7 of 8
ClearCorrect v. Align - IPR2025-00821

via thermocouples located on the top and bottom of the part. When the laminate has reached the desired temperature, the platens are opened, and the frame is moved from the flat portion of the mold to the forming portion, which in this case is a right angle bend. It should be noted that the top of the mold is attached to the upper hot platen via adjustable strapping allowing the mold to be opened and closed quickly. The mold is closed at the rate specified on the press controls after transfer has been completed. After a hold time of about 3 min, during which the strapping is removed, the mold can then be moved to the chilled platens for cooling. Once cool the part may be removed and inspected.

Using $[0/90/\pm45]_{2s}$ laminates, the maximum forming rate of 13.8 mm/s was found to cause wrinkling of plies on the inner radius of the part at a temperature of about 346°C. At this forming rate and temperature, the compressive stress in the 0° ply obtained from the forming model with the cylindrical bending assumption is 7.9 MPa. Forming laminates with the same lay-up at the same temperature, but at lower forming rates of 4.6 and 6.6 mm/s resulted in no ply wrinkling effects. As expected, forming at higher temperatures and at the maximum rate of 13.8 mm/s also did not result in any ply wrinkling. The stress of 7.9 MPa can be regarded as a critical stress of ply wrinkling at the forming temperature of 346°C. To avoid wrinkling, the forming rate must be such that the compressive stress in the ply of the inner radius is under this critical value. Apparently, this critical value is temperature dependent.

CONCLUSIONS

A forming model for thermoplastic composite laminates has been derived based upon Mindlin plate theory using transverse shear strain to account for interply slip deformation. The composite properties are assumed to be elastic–viscoplastic. The transverse shear property is derived from the interply slip behavior of the laminate. Such a model can be implemented in commercial finite element codes through the user subroutine to incorporate the viscoplastic constitutive model.

By using a simplifying assumption that is valid for fiber-dominated laminates, analytical solutions for three-point bending problems were obtained for AS4/PEEK thermoplastic composite laminates for various temperatures and loading rates. It was found that for a given forming rate (stroke rate), the present model predicted the forming load fairly close to that from the experimental data. It was also demonstrated that the present model can be used to design the forming rate to avoid occurrence of ply wrinkling during forming.

ACKNOWLEDGEMENT

This work is sponsored by the National Science Foundation Engineering Research Center for Intelligent Manufacturing Systems at Purdue University, West Lafayette, Indiana, USA.

REFERENCES

1 Kaprielian, P.V. and O'Neill, J.M. *Composites* 1989, **20**(1), 43–47
2 Tam, A.S. and Gutowski, T.G. *J. Compos. Mater.* 1989, **23**, 587–605
3 Spencer, A.J.M. 'Deformation of Fibre-Reinforced Materials', Clarendon Press, Oxford, 1972
4 Golden, K., Rogers, T.G. and Spencer, A.J.M. *Compos. Manuf.* 1991, **2**(3/4), 267–277
5 Rogers, T.G. and O'Neill, J.M. *Compos. Manuf.* 1991, **2**(3/4), 153–160
6 Pipkin, A.C. and Rogers, T.G. *J. Appl. Mech.* 1971, **38**, 634–640
7 Martin, T.A., Bhattacharyya, D. and Collins, I.F. *Compos. Manuf.* 1995, **6**(3–4), 177–187
8 Mindlin, R.D. *J. Appl. Mech.* 1951, **18**, 31–38
9 Whitney, J.M. and Pagano, N.J. *J. Appl. Mech.* 1970, **37**(4), 1031–1036
10 Gates, T.S. and Sun, C.T. *AIAA J.* 1991, **29**(3), 457–463
11 Morris, S.R. and Sun, C.T. *Compos. Manuf.* 1994, **5**(4), 217–224
12 Wang, C., Sun, C.T. and Gates, T.S. Elastic/Viscoplastic Behavior of Fiber Reinforced Thermoplastic Composites. In '31st AIAA/ASME/AHS/ASC Structures, Structural Dynamics, and Materials Conference', Long Beach, California, 2–4 April 1990, pp. 578–586
13 Chen, G. 'Nonlinear finite element analysis of plates and shells of composite laminates', *M.S. Thesis*, Purdue University, West Lafayette, Indiana, December 1988
14 Wang, C. 'Predictive forming of advanced thermoplastic composite structures', *Ph.D Dissertation*, Purdue University, West Lafayette, Indiana, December 1991
15 Mascia, L. 'Thermoplastics: Materials Engineering', 2nd edition, Elsevier Applied Science, London, 1989

ClearCorrect Exhibit 1165, Page 8 of 8
ClearCorrect v. Align - IPR2025-00821